# Supplementary Figure Legends

**Supplementary Figure S1 | Representative FACS plots for murine mammary stem cell experiments. a**, $CD24^{med}CD49f^{high}Lin^-$ mammary cells (mammary repopulating unit-containing population) and $CD24^{high}CD49f^{low}Lin^-$ cells (progenitor cell-containing population) were isolated by flow cytometry from 4 week old mice as described. Lineage markers included CD45, CD31, CD140a, and Ter119. In all cases, forward scatter area versus forward scatter width profiles were used to eliminate cell doublets and dead cells were eliminated by excluding $DAPI^+$ cells.

**Supplementary Figure S2 | Expression of ROS genes in human breast cancer subpopulations.** Gene Set Enrichment Analysis (GSEA) was used to analyze the enrichment of a curated list of genes involved in ROS metabolism using microarray gene expression data from sorted $CD44^+CD24^{-/low}Lin^-$ cells (cancer stem cell-containing population - CSC) and their non-tumorigenic counterparts (NTC). The GSEA enrichment plot is shown. $p < 0.001$.

**Supplementary Figure S3 | Isolation of $CD44^+CD24^{-/low}Lin^-$ CSC-enriched cells and non-tumorigenic cells from a human breast cancer. a,** FACS profile of human breast tumor from Fig. 1e. Lineage positive cells were excluded using CD45, CD3, CD10, CD64, CD31, and Glycophorin A. $CD44^+CD24^{-/low}Lin^-$ cells (cancer stem cell-enriched population) and non-tumorigenic cells were sorted using the indicated gates. **b**, Re-analysis of sorted $CD44^+CD24^{-/low}Lin^-$ cells. **c**, Re-analysis of sorted non-tumorigenic cells.

**Supplementary Figure S4 | Human cancer stem cell-enriched populations from some breast and head & neck carcinomas contain lower ROS concentrations than their respective non-tumorigenic cells. a**, FACS profile of human breast cancer from which $CD44^+CD24^{-/low}Lin^-$ cells (cancer stem cell-enriched population) and "Not $CD44^+CD24^{-/low}$" $Lin^-$ non-tumorigenic cells were isolated using flow cytometry. Lineage positive cells were excluded as in Supplementary Figure S3. Intracellular ROS concentrations were subsequently measured by DCF-DA staining. **b**, DCF-DA histograms for the two populations from **a**. **c**, FACS profile of human breast cancer from which $CD44^+CD24^{-/low}Lin^-$ cells and "Not $CD44^+CD24^{-/low}$" $Lin^-$ non-tumorigenic cells were isolated using flow cytometry. Lineage positive cells were excluded as in **a** with the addition of CD20. Intracellular ROS concentrations were subsequently measured by DCF-DA staining. **d**, DCF-DA histograms for the two populations from **c**. **e**, FACS profile of human head and neck cancer for which we analyzed intracellular ROS concentrations using DCF-DA staining. Lineage positive cells were excluded using CD45 and CD31. **f**, DCF-DA histograms for the two populations from **e**. In each case, the red gate/line represents the tumorigenic population and the green gate/line represents the non-tumorigenic population.

**Supplementary Figure S5 | Thy1$^{+}$CD24$^{+}$Lin$^{-}$ CSC-enriched cells from MMTV-*Wnt-1* breast tumors are enriched for cells with low intracellular ROS concentrations. a**, Thy1/CD24 FACS plot for representative MMTV-*Wnt-1* tumor with sort gates indicated. Lineage markers included CD45, CD31, and CD140a. In all cases, forward scatter area versus forward scatter width profiles were used to eliminate cell doublets and dead cells were eliminated by excluding DAPI$^{+}$ cells. **b**, Thy1$^{+}$CD24$^{+}$Lin$^{-}$ cells and "Not Thy1$^{+}$CD24$^{+}$" Lin$^{-}$ cells were isolated from MMTV-*Wnt-1* breast tumors by flow cytometry and ROS levels were analyzed as in Figure 1. The percentage of cells with low ROS concentrations was quantified within the two populations. Mean ± s.e.m. (n=7; *p*=0.003).

**Supplementary Figure S6 | Thy1$^{+}$CD24$^{+}$Lin$^{-}$ breast cancer cells develop less DNA damage after *in vitro* irradiation than non-tumorigenic cells.** Thy1$^{+}$CD24$^{+}$Lin$^{-}$ CSC-enriched cells and "Not Thy1$^{+}$CD24$^{+}$" Lin$^{-}$ non-tumorigenic cells from MMTV-*Wnt-1* breast tumors that were irradiated *in vitro* in bulk with 1 Gy of IR. The two populations were then sorted using flow cytometry and the resulting cells were immunostained for γ-H2AX. The percentage of cells with nuclear foci was quantified. One of two representative experiments is shown.

**Supplementary Figure S7 | Thy1$^{+}$CD24$^{+}$Lin$^{-}$ CSC-enriched breast cancer cells are relatively radioresistant *in vitro* compared to non-tumorigenic cells.** Clonogenic survival of Thy1$^{+}$CD24$^{+}$Lin$^{-}$ CSC-enriched cells and "Not Thy1$^{+}$CD24$^{+}$" Lin$^{-}$ non-tumorigenic cells before and after 2, 3, and 4 Gy of ionizing radiation. Mean ± s.e.m. One of three representative experiments is shown.

**Supplementary Table 1 | Transplantation of MRU-enriched cells based on intracellular levels of ROS.** CD24$^{med}$CD49f$^{high}$Lin$^{-}$ mammary cells (enriched for mammary repopulating units) were isolated from mammary fat pads from C57Bl/6J female mice and were immediately loaded with 10 μM DCF-DA. Labeled cells were then re-sorted into "ROS-low" and "ROS-mid" sub-populations based on their DCF-DA staining profile (in comparison to that of CD24$^{high}$CD49f$^{low}$Lin$^{-}$ progenitor cells, which displayed a "ROS-high" profile). Sorted cells (500-5000 depending on experiment) were injected into cleared mammary fat pads of 21-day-old female C57Bl/6J mice and were scored by wholemount analysis 5–6 weeks later.

**Supplementary Table 2 | ROS metabolism genes are overrepresented in breast CSC signatures compared with NTC signatures.** Gene Set Enrichment Analysis (GSEA) was used to analyze the enrichment of a curated list of genes involved in ROS metabolism using microarray gene expression data from sorted CD44$^{+}$CD24$^{-/low}$Lin$^{-}$ cells (cancer stem cell-containing population) and their non-tumorigenic counterparts. GSEA leading edge analysis identified the indicated genes as being the core enriched genes.

**Supplementary Table 3 | Transplantation of MMTV-*Wnt-1* tumor cells based on intracellular levels of ROS.** $Lin^-$ or $Thy1^+CD24^+Lin^-$ cells from MMTV-*Wnt-1* tumors were sorted and then immediately loaded with 10 μM DCF-DA as described. Labeled cells were then re-sorted into “ROS-low” and “ROS-high” sub-populations based on their DCF-DA staining profile. Sorted cells (100-1000 depending on experiment) were injected into syngeneic recipients and tumor formation was scored.

**Supplementary Table 4 | List of genes involved in ROS metabolism.** We based our ROS gene list on a recently published gene list by Tothova et al. This list was initially generated by identifying genes annotated with the following biological process GeneOntology terms: response to oxidative stress; response to reactive oxygen species; response to hydrogen peroxide; response to oxygen radical; and response to superoxide. We further manually curated this list by removing all genes for which we could not find at least one publication in PubMed providing evidence for an ROS association. The resulting gene list consisted of 36 genes and was used for the GSEA analysis described in the text.

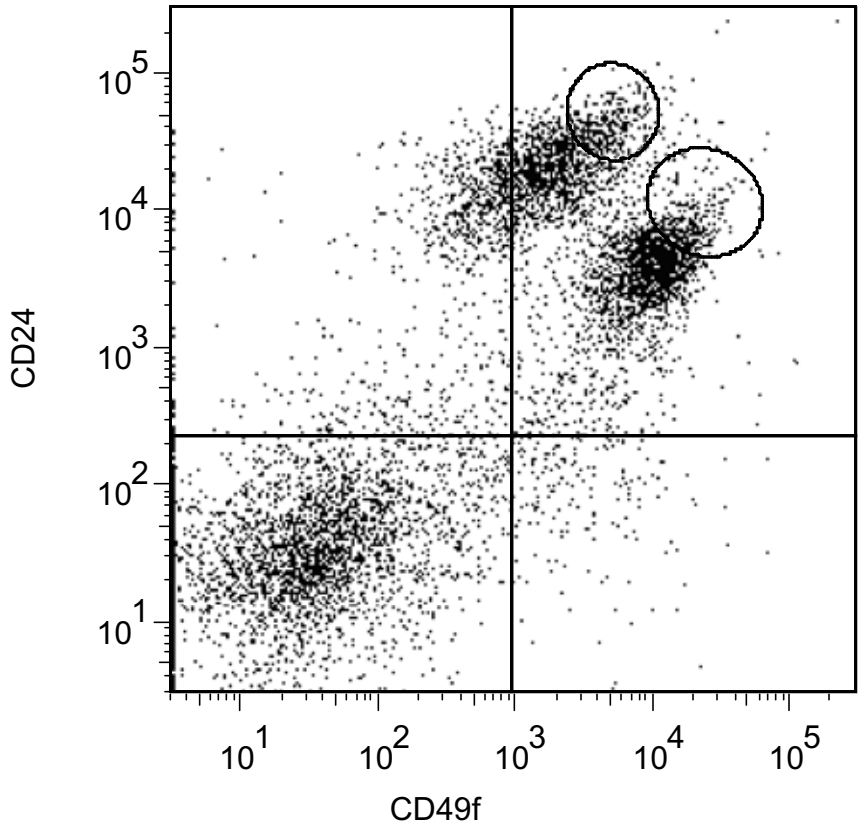


**Supplementary Fig. S1**

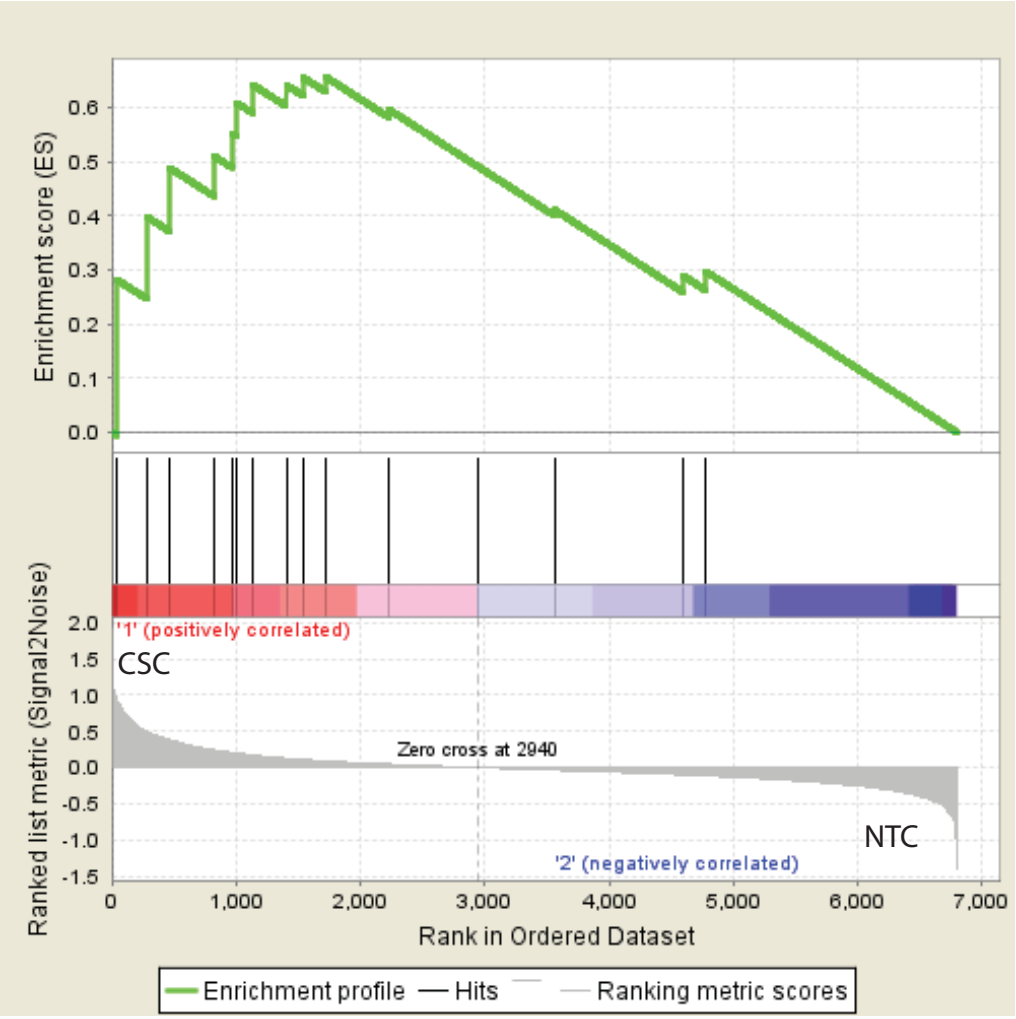


**Supplementary Fig. S2**

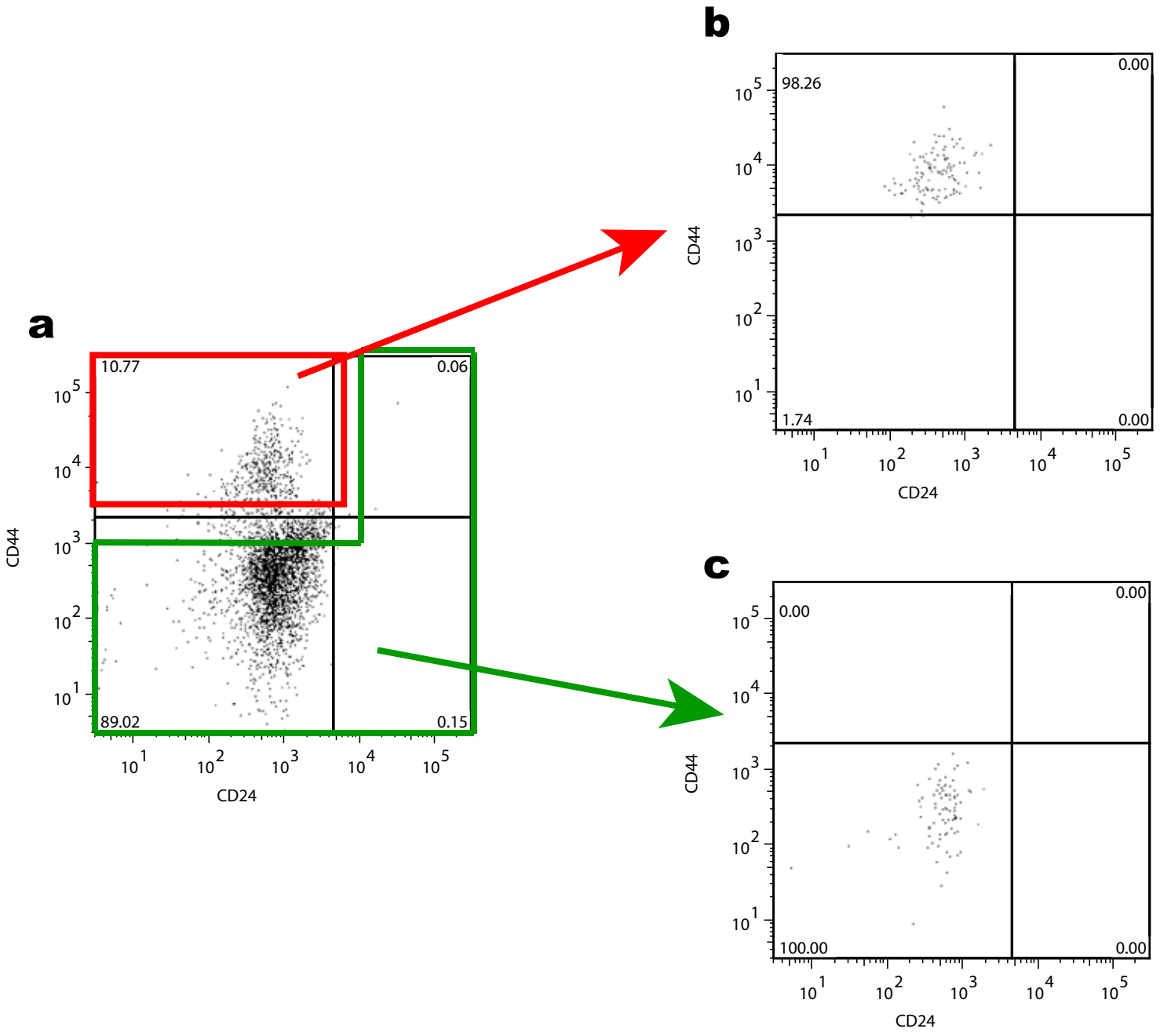


**Supplementary Fig. S3**

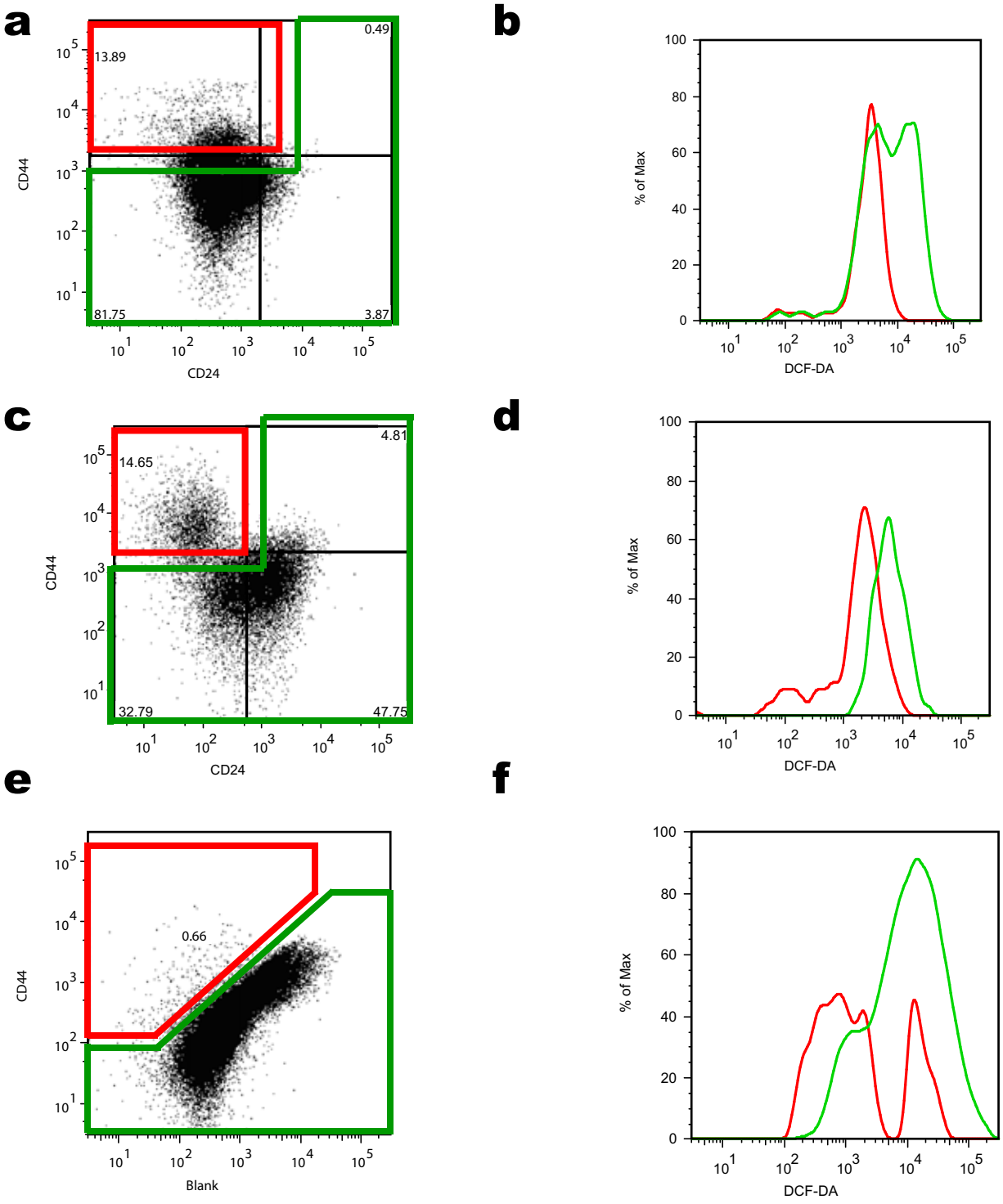


**Supplementary Fig. S4**

**a**

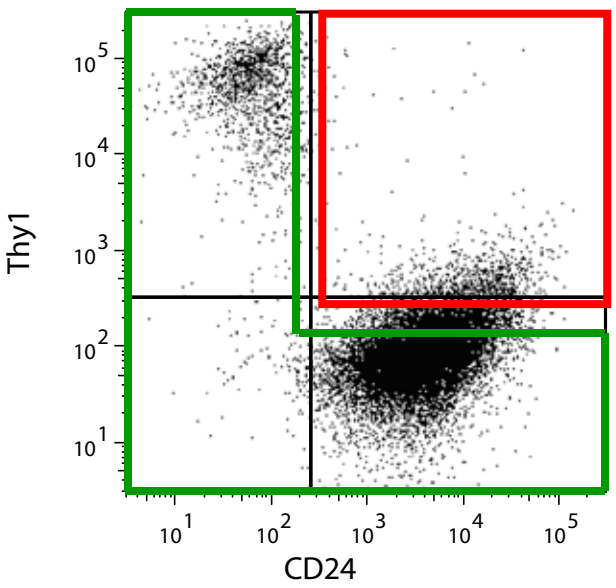


**Thy1+ CD24+ Lin- cells (tumorigenic)**

**“Not Thy1+CD24+" Lin- cells (non-tumorigenic)**

**b**

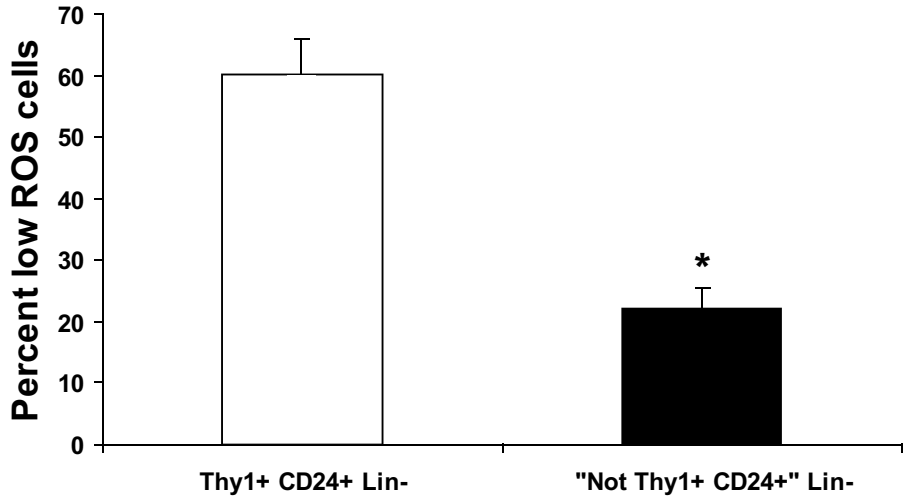


**Supplementary Fig. S5**

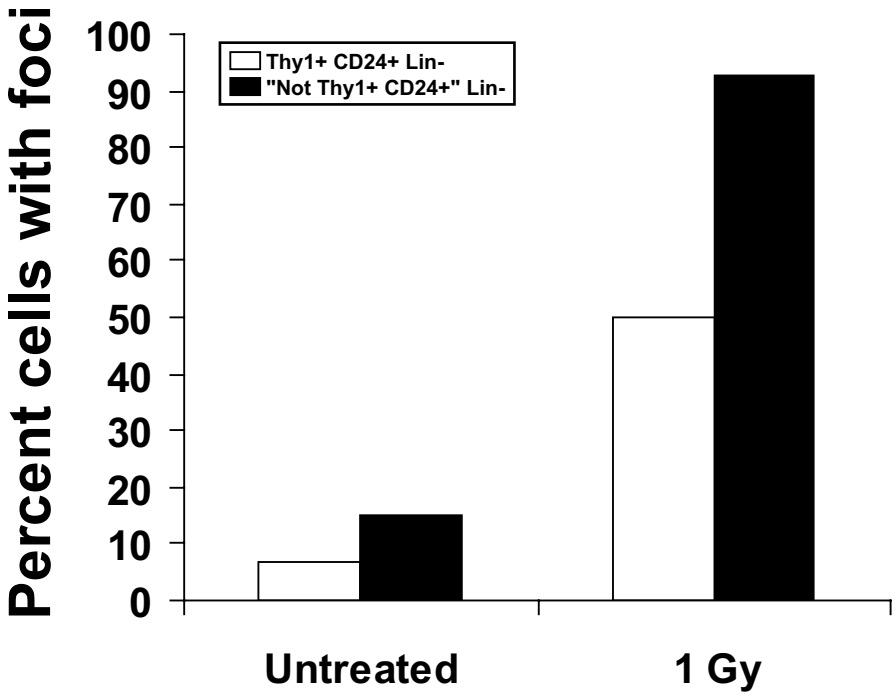


**Supplementary Fig. S6**

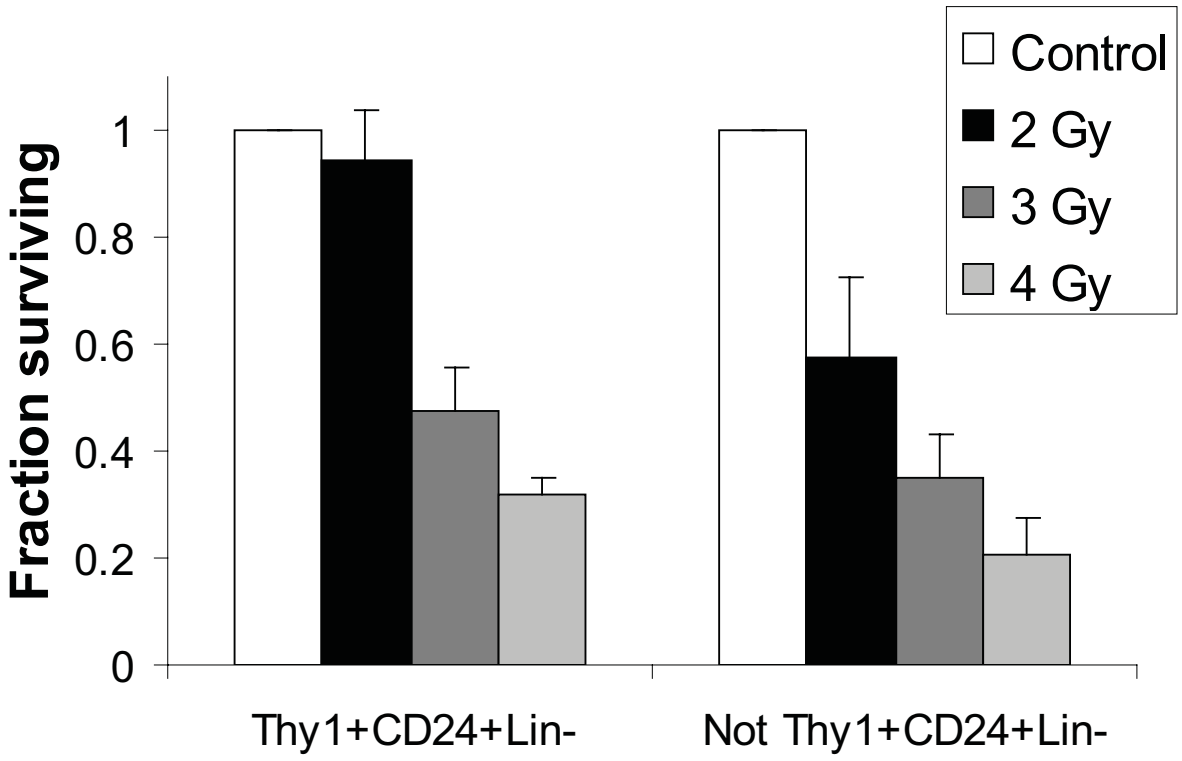


**Supplementary Fig. S7**

**Supplementary Table 1:**

| Phenotype | No. of positive pads / total injections |
|---|---|
| | |
| ROS low | 3/8 |
| | |
| ROS medium | 4/7 |
| | |

**Supplementary Table 2:**

| Probe Set ID | Gene Symbol |
|---|---|
| | |
| 203028_s_at | CYBA |
| 201300_s_at | PRNP |
| 219281_at | MSRA |
| 200736_s_at | GPX1 |
| 201010_s_at | TXNIP |
| 215223_s_at | SOD2 |
| 201432_at | CAT |
| 205672_at | XPA |
| 201193_at | IDH1 |
| 201106_at | GPX4 |

**Supplementary Table 3**:

| ROS Phenotype (of $Lin^-$) | No. of tumors / total injections |
|---|---|
| | |
| Bottom 25% ROS | 2/14 |
| | |
| Top 25% ROS | 4/15 |
| | |

| ROS Phenotype (of $Thy1^+CD24^+Lin^-$) | No. of tumors / total injections |
|---|---|
| | |
| ROS low | 5/10 |
| | |
| ROS high | 5/7 |
| | |

## Supplementary Table 4:

| Symbol | Name |
|---|---|
| AASS | Aminoadipate-semialdehyde synthase |
| ALS2 | Amyotrophic lateral sclerosis 2 (juvenile) |
| APOE | Apolipoprotein E |
| CAT | Catalase |
| CCS | Copper chaperone for superoxide dismutase |
| CYBA | Cytochrome b-245, alpha polypeptide |
| EPX | Eosinophil peroxidase |
| ERCC6 | Excision repair cross-complementing rodent repair deficiency, complementation group 6 |
| GAB1 | GRB2-associated binding protein 1 |
| GPX1 | Glutathione peroxidase 1 |
| GPX2 | Glutathione peroxidase 2 (gastrointestinal) |
| GPX3 | Glutathione peroxidase 3 (plasma) |
| GPX4 | Glutathione peroxidase 4 (phospholipid hydroperoxidase) |
| GPX5 | Glutathione peroxidase 5 (epididymal androgen-related protein) |
| GPX6 | Glutathione peroxidase 6 (olfactory) |
| GPX7 | Glutathione peroxidase 7 |
| IDH1 | Isocitrate dehydrogenase 1 (NADP+), soluble |
| MPO | Myeloperoxidase |
| MSRA | Methionine sulfoxide reductase A |
| NCF2 | Neutrophil cytosolic factor 2 (65kDa, chronic granulomatous disease, autosomal 2) |
| NOX4 | NADPH oxidase 4 |
| NOXO1 | NADPH oxidase organizer 1 |
| PPP1R15B | Protein phosphatase 1, regulatory (inhibitor) subunit 15B |
| PRDX1 | Peroxiredoxin 1 |
| PRDX2 | Peroxiredoxin 2 |
| PRDX6 | Peroxiredoxin 6 |
| PRDX6-RS1 | Peroxiredoxin 6, related sequence 1 |
| PRNP | Prion protein (p27-30) |
| SOD1 | Superoxide dismutase 1, soluble (amyotrophic lateral sclerosis 1 (adult)) |
| SOD2 | Superoxide dismutase 2, mitochondrial |
| SOD3 | Superoxide dismutase 3, extracellular |
| TPO | Thyroid peroxidase |
| TXNIP | Thioredoxin interacting protein |
| TXNRD2 | Thioredoxin reductase 2 |
| UCP3 | Uncoupling protein 3 (mitochondrial, proton carrier) |
| XPA | Xeroderma pigmentosum, complementation group A |